Limits on Gravitational-Wave Emission from Selected Pulsars Using LIGO Data

B. Abbott,[11] R. Abbott,[14] R. Adhikari,[12] A. Ageev,[19,26] B. Allen,[38] R. Amin,[33] S. B. Anderson,[11] W. G. Anderson,[28] M. Araya,[11] H. Armandula,[11] M. Ashley,[27] F. Asiri,[11] P. Aufmuth,[30] C. Aulbert,[1] S. Babak,[7] R. Balasubramanian,[7] S. Ballmer,[12] B. C. Barish,[11] C. Barker,[13] D. Barker,[13] M. Barnes,[11] B. Barr,[34] M. A. Barton,[11] K. Bayer,[12] R. Beausoleil,[25] K. Belczynski,[22] R. Bennett,[34] S. J. Berukoff,[1] J. Betzwieser,[12] B. Bhawal,[11] I. A. Bilenko,[19] G. Billingsley,[11] E. Black,[11] K. Blackburn,[11] L. Blackburn,[12] B. Bland,[13] B. Bochner,[12] L. Bogue,[11] R. Bork,[11] S. Bose,[39] P. R. Brady,[38] V. B. Braginsky,[19] J. E. Brau,[36] D. A. Brown,[38] A. Bullington,[25] A. Bunkowski,[2,30] A. Buonanno,[6] R. Burgess,[12] D. Busby,[11] W. E. Butler,[37] R. L. Byer,[25] L. Cadonati,[12] G. Cagnoli,[34] J. B. Camp,[20] C. A. Cantley,[34] L. Cardenas,[11] K. Carter,[14] M. M. Casey,[34] J. Castiglione,[33] A. Chandler,[11] J. Chapsky,[11] P. Charlton,[11] S. Chatterji,[12] S. Chelkowski,[2,30] Y. Chen,[6] V. Chickarmane,[15] D. Chin,[35] N. Christensen,[8] D. Churches,[7] T. Cokelaer,[7] C. Colacino,[32] R. Coldwell,[33] M. Coles,[14] D. Cook,[13] T. Corbitt,[12] D. Coyne,[11] J. D. E. Creighton,[38] T. D. Creighton,[11] D. R. M. Crooks,[34] P. Csatorday,[12] B. J. Cusack,[3] C. Cutler,[1] E. D'Ambrosio,[11] K. Danzmann,[2,30] E. Daw,[15] D. DeBra,[25] T. Delker,[33] V. Dergachev,[35] R. DeSalvo,[11] S. Dhurandhar,[10] A. Di Credico,[26] M. Díaz,[28] H. Ding,[11] R. W. P. Drever,[4] R. J. Dupuis,[34] J. A. Edlund,[11] P. Ehrens,[11] E. J. Elliffe,[34] T. Etzel,[11] M. Evans,[11] T. Evans,[14] S. Fairhurst,[38] C. Fallnich,[30] D. Farnham,[11] M. M. Fejer,[25] T. Findley,[24] M. Fine,[11] L. S. Finn,[27] K. Y. Franzen,[33] A. Freise,[2] R. Frey,[36] P. Fritschel,[12] V. V. Frolov,[14] M. Fyffe,[14] K. S. Ganezer,[5] J. Garofoli,[13] J. A. Giaime,[15] A. Gillespie,[11] K. Goda,[12] G. González,[15] S. Goßler,[30] P. Grandclément,[22] A. Grant,[34] C. Gray,[13] A. M. Gretarsson,[14] D. Grimmett,[11] H. Grote,[2] S. Grunewald,[1] M. Guenther,[13] E. Gustafson,[25] R. Gustafson,[35] W. O. Hamilton,[15] M. Hammond,[14] J. Hanson,[14] C. Hardham,[25] J. Harms,[18] G. Harry,[12] A. Hartunian,[11] J. Heefner,[11] Y. Hefetz,[12] G. Heinzel,[2] I. S. Heng,[30] M. Hennessy,[25] N. Hepler,[27] A. Heptonstall,[34] M. Heurs,[30] M. Hewitson,[2] S. Hild,[2] N. Hindman,[13] P. Hoang,[11] J. Hough,[34] M. Hrynevych,[11] W. Hua,[25] M. Ito,[36] Y. Itoh,[1] A. Ivanov,[11] O. Jennrich,[34] B. Johnson,[13] W. W. Johnson,[15] W. R. Johnston,[28] D. I. Jones,[27] L. Jones,[11] D. Jungwirth,[11] V. Kalogera,[22] E. Katsavounidis,[12] K. Kawabe,[13] S. Kawamura,[21] W. Kells,[11] J. Kern,[14] A. Khan,[14] S. Killbourn,[34] C. J. Killow,[34] C. Kim,[22] C. King,[11] P. King,[11] S. Klimenko,[33] S. Koranda,[38] K. Kötter,[30] J. Kovalik,[14] D. Kozak,[11] B. Krishnan,[1] M. Landry,[13] J. Langdale,[14] B. Lantz,[25] R. Lawrence,[12] A. Lazzarini,[11] M. Lei,[11] I. Leonor,[36] K. Libbrecht,[11] A. Libson,[8] P. Lindquist,[11] S. Liu,[11] J. Logan,[11] M. Lormand,[14] M. Lubinski,[13] H. Lück,[2,30] T. T. Lyons,[11] B. Machenschalk,[1] M. MacInnis,[12] M. Mageswaran,[11] K. Mailand,[11] W. Majid,[11] M. Malec,[2,30] F. Mann,[11] A. Marin,[12] S. Márka,[11] E. Maros,[11] J. Mason,[11] K. Mason,[12] O. Matherny,[13] L. Matone,[13] N. Mavalvala,[12] R. McCarthy,[13] D. E. McClelland,[3] M. McHugh,[17] J. W. C. McNabb,[27] G. Mendell,[13] R. A. Mercer,[32] S. Meshkov,[11] E. Messaritaki,[38] C. Messenger,[32] V. P. Mitrofanov,[19] G. Mitselmakher,[33] R. Mittleman,[12] O. Miyakawa,[11] S. Miyoki,[11] S. Mohanty,[28] G. Moreno,[13] K. Mossavi,[2] G. Mueller,[33] S. Mukherjee,[28] P. Murray,[34] J. Myers,[13] S. Nagano,[2] T. Nash,[11] R. Nayak,[10] G. Newton,[34] F. Nocera,[11] J. S. Noel,[39] P. Nutzman,[22] T. Olson,[23] B. O'Reilly,[14] D. J. Ottaway,[12] A. Ottewill,[38] D. Ouimette,[11] H. Overmier,[14] B. J. Owen,[27] Y. Pan,[6] M. A. Papa,[1] V. Parameshwaraiah,[13] C. Parameswariah,[14] M. Pedraza,[11] S. Penn,[9] M. Pitkin,[34] M. Plissi,[34] R. Prix,[1] V. Quetschke,[33] F. Raab,[13] H. Radkins,[13] R. Rahkola,[36] M. Rakhmanov,[33] S. R. Rao,[11] K. Rawlins,[12] S. Ray-Majumder,[38] V. Re,[32] D. Redding,[11] M. W. Regehr,[11] T. Regimbau,[7] S. Reid,[34] K. T. Reilly,[11] K. Reithmaier,[11] D. H. Reitze,[33] S. Richman,[12] R. Riesen,[14] K. Riles,[35] B. Rivera,[13] A. Rizzi,[14] D. I. Robertson,[34] N. A. Robertson,[25,34] L. Robison,[11] S. Roddy,[14] J. Rollins,[12] J. D. Romano,[7] J. Romie,[11] H. Rong,[33] D. Rose,[11] E. Rotthoff,[27] S. Rowan,[34] A. Rüdiger,[2] P. Russell,[11] K. Ryan,[13] I. Salzman,[11] V. Sandberg,[13] G. H. Sanders,[11] V. Sannibale,[11] B. Sathyaprakash,[7] P. R. Saulson,[26] R. Savage,[13] A. Sazonov,[33] R. Schilling,[2] K. Schlaufman,[27] V. Schmidt,[11] R. Schnabel,[18] R. Schofield,[36] B. F. Schutz,[1,7] P. Schwinberg,[13] S. M. Scott,[3] S. E. Seader,[39] A. C. Searle,[3] B. Sears,[11] S. Seel,[11] F. Seifert,[18] A. S. Sengupta,[10] C. A. Shapiro,[27] P. Shawhan,[11] D. H. Shoemaker,[12] Q. Z. Shu,[33] A. Sibley,[14] X. Siemens,[38] L. Sievers,[11] D. Sigg,[13] A. M. Sintes,[1,31] J. R. Smith,[2] M. Smith,[12] M. R. Smith,[11] P. H. Sneddon,[34] R. Spero,[11] G. Stapfer,[14] D. Steussy,[8] K. A. Strain,[34] D. Strom,[36] A. Stuver,[27] T. Summerscales,[27] M. C. Sumner,[11] P. J. Sutton,[11] J. Sylvestre,[11] A. Takamori,[11] D. B. Tanner,[33] H. Tariq,[11] I. Taylor,[7] R. Taylor,[11] R. Taylor,[34] K. A. Thorne,[27] K. S. Thorne,[6] M. Tibbits,[27] S. Tilav,[11] M. Tinto,[4] K. V. Tokmakov,[19] C. Torres,[20] C. Torrie,[11] G. Traylor,[14] W. Tyler,[11] D. Ugolini,[29] C. Ungarelli,[32] M. Vallisneri,[6] M. van Putten,[12] S. Vass,[11] A. Vecchio,[32] J. Veitch,[34] C. Vorvick,[13] S. P. Vyachanin,[19] L. Wallace,[11] H. Walther,[18] H. Ward,[34] B. Ware,[11] K. Watts,[14] D. Webber,[11] A. Weidner,[18] U. Weiland,[30] A. Weinstein,[11] R. Weiss,[12] H. Welling,[30] L. Wen,[11] S. Wen,[15] J. T. Whelan,[17] S. E. Whitcomb,[11] B. F. Whiting,[33] S. Wiley,[5] C. Wilkinson,[13] P. A. Willems,[11] P. R. Williams,[1] R. Williams,[4] B. Willke,[30] A. Wilson,[11] B. J. Winjum,[27] W. Winkler,[2] S. Wise,[33] A. G. Wiseman,[38] G. Woan,[34] R. Wooley,[14] J. Worden,[13] W. Wu,[33] I. Yakushin,[14] H. Yamamoto,[11]

 © 2005 The American Physical Society

S. Yoshida,[24] K. D. Zaleski,[27] M. Zanolin,[12] I. Zawischa,[30] L. Zhang,[11] R. Zhu,[1] N. Zotov,[16] M. Zucker,[14] and J. Zweizig[11]

(LIGO Scientific Collaboration)*

[1]*Albert-Einstein-Institut, Max-Planck-Institut für Gravitationsphysik, D-14476 Golm, Germany*
[2]*Albert-Einstein-Institut, Max-Planck-Institut für Gravitationsphysik, D-30167 Hannover, Germany*
[3]*Australian National University, Canberra, 0200, Australia*
[4]*California Institute of Technology, Pasadena, California 91125, USA*
[5]*California State University Dominguez Hills, Carson, California 90747, USA*
[6]*Caltech-CaRT, Pasadena, California 91125, USA*
[7]*Cardiff University, Cardiff, CF2 3YB, United Kingdom*
[8]*Carleton College, Northfield, Minnesota 55057, USA*
[9]*Hobart and William Smith Colleges, Geneva, New York 14456, USA*
[10]*Inter-University Centre for Astronomy and Astrophysics, Pune-411007, India*
[11]*LIGO-California Institute of Technology, Pasadena, California 91125, USA*
[12]*LIGO-Massachusetts Institute of Technology, Cambridge, Massachusetts 02139, USA*
[13]*LIGO Hanford Observatory, Richland, Washington 99352, USA*
[14]*LIGO Livingston Observatory, Livingston, Louisiana 70754, USA*
[15]*Louisiana State University, Baton Rouge, Louisiana 70803, USA*
[16]*Louisiana Tech. University, Ruston, Louisiana 71272, USA*
[17]*Loyola University, New Orleans, Louisiana 70118, USA*
[18]*Max Planck Institut für Quantenoptik, D-85748, Garching, Germany*
[19]*Moscow State University, Moscow, 119992, Russia*
[20]*NASA/Goddard Space Flight Center, Greenbelt, Maryland 20771, USA*
[21]*National Astronomical Observatory of Japan, Tokyo 181-8588, Japan*
[22]*Northwestern University, Evanston, Illinois 60208, USA*
[23]*Salish Kootenai College, Pablo, Montana 59855, USA*
[24]*Southeastern Louisiana University, Hammond, Louisiana 70402, USA*
[25]*Stanford University, Stanford, California 94305, USA*
[26]*Syracuse University, Syracuse, New York 13244, USA*
[27]*The Pennsylvania State University, University Park, Pennsylvania 16802, USA*
[28]*The University of Texas at Brownsville and Texas Southmost College, Brownsville, Texas 78520, USA*
[29]*Trinity University, San Antonio, Texas 78212, USA*
[30]*Universität Hannover, D-30167 Hannover, Germany*
[31]*Universitat de les Illes Balears, E-07122 Palma de Mallorca, Spain*
[32]*University of Birmingham, Birmingham, B15 2TT, United Kingdom*
[33]*University of Florida, Gainesville, Florida 32611, USA*
[34]*University of Glasgow, Glasgow, G12 8QQ, United Kingdom*
[35]*University of Michigan, Ann Arbor, Michigan 48109, USA*
[36]*University of Oregon, Eugene, Oregon 97403, USA*
[37]*University of Rochester, Rochester, New York 14627, USA*
[38]*University of Wisconsin-Milwaukee, Milwaukee, Wisconsin 53201, USA*
[39]*Washington State University, Pullman, Washington 99164, USA*

M. Kramer and A. G. Lyne

University of Manchester, Jodrell Bank Observatory, Macclesfield, Cheshire, SK11 9DL, United Kingdom
(Received 29 October 2004; published 12 May 2005)

We place direct upper limits on the amplitude of gravitational waves from 28 isolated radio pulsars by a coherent multidetector analysis of the data collected during the second science run of the LIGO interferometric detectors. These are the first *direct* upper limits for 26 of the 28 pulsars. We use coordinated radio observations for the first time to build radio-guided phase templates for the expected gravitational-wave signals. The unprecedented sensitivity of the detectors allows us to set strain upper limits as low as a few times 10^{-24}. These strain limits translate into limits on the equatorial ellipticities of the pulsars, which are smaller than 10^{-5} for the four closest pulsars.

DOI: 10.1103/PhysRevLett.94.181103 PACS numbers: 04.80.Nn, 07.05.Kf, 95.55.Ym, 97.60.Gb

A worldwide effort is underway to detect gravitational waves (GWs) and thus test a fundamental prediction of general relativity. In preparation for long-term operations, the Laser Interferometric Gravitational Wave Observatory

(LIGO) and GEO experiments conducted their first science run (S1) during 17 days in 2002. The detectors and the pulsar analysis of the S1 data are described in [1,2], respectively. LIGO's second science run (S2) was carried out from 14 February to 14 April 2003, with dramatically improved sensitivity compared to S1. During S2 the GEO detector was not operating.

A spinning neutron star is expected to emit GWs if it is not perfectly symmetric about its rotation axis. The strain amplitude h_0 of the emitted signal is proportional to the star's deformation as measured by its ellipticity ϵ [3]. Using data from S2, this Letter reports *direct* observational limits on the GW emission and corresponding ellipticities from the 28 most rapidly rotating isolated pulsars for which radio data are complete enough to guide the phase of our filters with sufficient precision. These are the first such limits for 26 of the pulsars.

The limits reported here are still well above the indirect limits inferred from observed pulsar spin-down, where available (Fig. 1). However, fourteen of our pulsars are in globular clusters, where local gravitational accelerations produce Doppler effects that mask the intrinsic pulsar spin-down, sometimes even producing apparent spin-up. For these pulsars our observations therefore place the first limits that are inherently independent of cluster dynamics, albeit at levels well above what one would expect if all globular cluster pulsars are similar to field pulsars.

Our most stringent ellipticity upper limit is 4.5×10^{-6}. While still above the maximum expected from conventional models of nuclear matter, distortions of this size would be permitted within at least one exotic theory of neutron star structure [4].

Detectors.—Each of LIGO's three detectors is a power-recycled Michelson interferometer with Fabry-Perot cavities in the long arms [1]. Two detectors, the 4 km arm H1 and the 2 km arm H2 detectors, are collocated in Hanford, WA. The 4 km arm L1 detector is situated in Livingston Parish, LA. Improvements in noise performance between S1 and S2 were approximately an order of magnitude over a broad frequency range. Modifications that were made between S1 and S2 to aid in noise reduction and improve stability include (i) increased laser power to reduce high-frequency noise, (ii) better angular control of the mirrors of the interferometer, and (iii) the use of lower noise digital test mass suspension controllers in all detectors.

During S2, the LIGO detectors' noise performance in the band 40–2000 Hz was better than any previous interferometer. The best strain sensitivity, achieved by L1, was $\sim 3 \times 10^{-22}$ Hz$^{-1/2}$ near 200 Hz, translating via Eq. (2.2) of [2] to a detectable amplitude for a continuous signal of about 3×10^{-24}, as shown in Fig. 1. The relative timing stability between the interferometers was also significantly improved. Monitored with GPS-synchronized clocks to be better than 10 μs over S2, it allowed the coherent combination of the strain data of all three detectors to form joint upper limits.

Analysis method.—In [2] a search for gravitational waves from the millisecond pulsar J1939 + 2134 using S1 data was presented. In that work, two different data analysis methods were used, one in the time domain and the other in the frequency domain. Here we extend the former method [2,5] and apply it to 28 isolated pulsars.

Following [2] we model the sources as nonprecessing triaxial neutron stars showing the same rotational phase evolution as is present in the radio signal and perform a complex heterodyne of the strain data from each detector at the instantaneous frequency of the expected gravitational-wave signal, which is twice the observed radio rotation frequency. These data are then down-sampled to 1/60 Hz and are referred to as B_k. Any gravitational signal in the data would show a residual time evolution reflecting the antenna pattern of the detector, varying over the day as the source moved through the pattern, but with a functional form that depended on several other source-observer parameters: the antenna responses to plus and cross polarizations, the amplitude of the gravitational wave h_0, the angle between the line of sight to the pulsar and its spin axis ι, the polarization angle of the gravitational radiation ψ (all defined in [3]), and the phase ϕ_0 of the gravitational-wave signal at some fiducial time t_0. Let $\boldsymbol{a}$ be a vector in parameter space with components (h_0, ι, ψ, ϕ_0).

The analysis proceeds by determining the posterior probability distribution function (PDF) of $\boldsymbol{a}$ given the data B_k and the signal model:

$$p(\boldsymbol{a}|\{B_k\}) \propto p(\boldsymbol{a})p(\{B_k\}|\boldsymbol{a}), \tag{1}$$

where $p(\{B_k\}|\boldsymbol{a})$ is the likelihood and $p(\boldsymbol{a})$ the prior PDF we assign to the model parameters. We have used a uniform prior for $\cos\iota$, ϕ_0, ψ, and h_0 ($h_0 > 0$), in common with [2]. A uniform prior for h_0 has been chosen for its simplicity and for the easy comparison of our results to other observations. This prior favors high values of h_0 (which comprise the majority of the parameter space) and therefore generates a somewhat conservative upper limit for its value. Indeed, the reader might prefer to regard our resulting posterior PDFs for h_0 as marginalized likelihoods rather than probabilities for h_0—these are functionally identical using our priors.

As in [2] we use a Gaussian joint likelihood for $p(\{B_k\}|\boldsymbol{a})$. In [2] the S1 noise floor was estimated over a 60 s period from a 4 Hz band about the expected signal frequency. This gave a reliable point estimate for the noise level but was sensitive to spectral contamination within the band, as demonstrated in the analysis of the GEO S1 data. In this Letter we exploit the improved stationarity of the instruments that make it reasonable to assume the noise floor is constant over periods of 30 min [5]. In addition, we restrict the bandwidth to 1/60 Hz, which makes it possible to search for signals from pulsars at frequencies close to

strong spectral disturbances. However, the noise level now determined is less certain as the estimate relies on fewer data. We take account of this increased uncertainty by explicitly marginalizing with a Jeffreys prior over the constant but unknown noise level for each 30 min period of data [6]. The likelihood for this analysis is then the combined likelihood for all the 30 min stretches of data, labeled by j in Eq. (2), taken as independent:

$$p(\{B_k\}|\boldsymbol{a}) \propto \prod_j \Big(\sum_{k=k_{1(j)}}^{k_{2(j)}} |B_k - y_k|^2 \Big)^{-m}, \qquad (2)$$

where y_k is the signal model given by Eq. (4.10) in [2] and $m = k_{2(j)} - k_{1(j)} + 1 = 30$ is the number of B_k data points in a 30 min segment.

In principle the period over which the data are assumed stationary need not be fixed, and can be adjusted dynamically to reflect instrumental performance over the run. We have limited our analysis to continuous 30 min stretches of data, which included more than 88% of the S2 science data set. Inclusion of shorter data sections would at best have resulted in a ~6% improvement on the strain upper limits reported here.

Validation by hardware injections.—The software was validated by checking its performance on fake pulsar signals injected in artificial and real detector noise, both in software [2] and in hardware. In particular, two artificial signals (P1, P2) were added digitally to the interferometer length sensing and control systems (responsible for maintaining a given interferometer on resonance), resulting in a differential length dither in the optical cavities of the detector. These injections were designed to give an end-to-end validation of the search pipeline starting from as far up the observing chain as possible.

The pulsar signals were injected for 12 h at frequencies of 1279.123 Hz (P1) and 1288.901 Hz (P2) with frequency derivatives of zero and -10^{-8} Hz s^{-1}, respectively, and strain amplitudes of 2×10^{-21}. In the case of the 4 km instruments, the displacement induced by this strain was up to $4000\ \mathrm{m} \times 2 \times 10^{-21} = 8 \times 10^{-18}$ m. These give signal-to-noise ratios [as defined by Eq. (79) of [3]] of 26 and 40 for P1 in H1 and L1, respectively, and of 38 and 34 for P2. The signals were modulated and Doppler shifted to simulate sources at fixed positions on the sky with $\psi = 0$, $\cos\iota = 0$, and $\phi_0 = 0$. To illustrate, posterior PDFs for the recovered P1 signal are shown in Fig. 2. The results derived from the different detectors are in broad statistical agreement, confirming that the relative calibrations are consistent and that the assessments of uncertainty (expressed in the posterior widths) are reasonable. Results for P2 were very similar to these.

The phase stability of the detectors in S2 allowed us to implement a *joint* coherent analysis based on data from all three participating instruments. This technique was noted in [2], but could not be performed on the S1 data because of timing uncertainties that existed when those observations

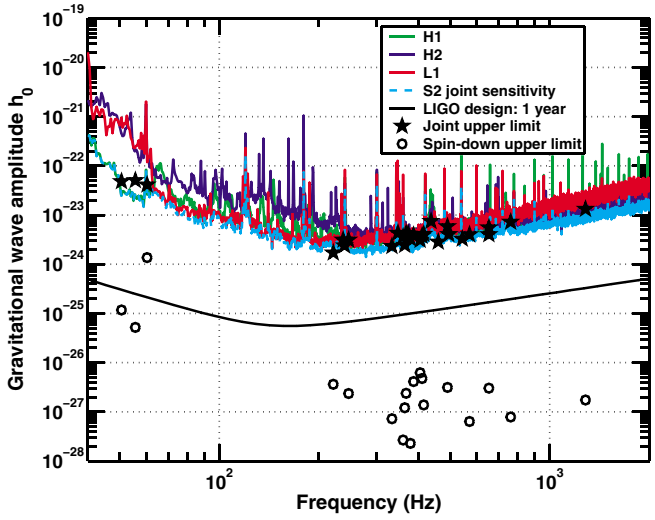

FIG. 1 (color). Upper curves: h_0 amplitudes detectable from a known generic source with a 1% false alarm rate and 10% false dismissal rate, as given by Eq. (2.2) in [2] for single detector analyses and for a joint detector analysis. All the curves use typical S2 sensitivities and observation times. Lower curve: LIGO design sensitivity for 1 yr of data. Stars: upper limits found in this Letter for 28 known pulsars. Circles: spin-down upper limits for the pulsars with negative frequency derivative values if *all* the measured rotational energy loss were due to gravitational waves and assuming a moment of inertia of 10^{45} g cm^2.

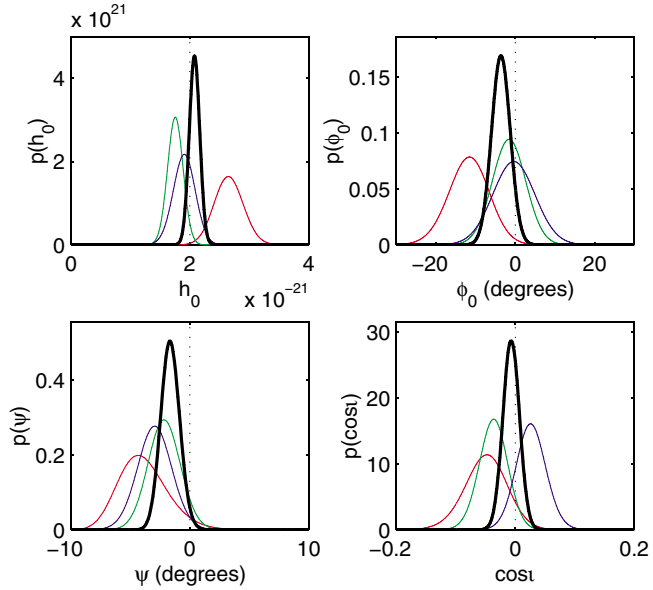

FIG. 2 (color). Marginalized PDFs for the parameters of the artificial pulsar P1. The vertical dotted lines show the values used to generate the signal, the colored lines show the results from the individual detectors (H1 green, H2 blue, L1 red), and the black lines show the joint result from combining coherently data from all three.

TABLE I. The 28 pulsars targeted in the S2 run, with approximate spin parameters. The right-hand two columns show the 95% upper limit on h_0 and ellipticity. These upper limits do *not* include the uncertainties due to calibration and to pulsar timing accuracy, which are discussed in the text, nor uncertainties in the pulsar's distance, r.

Pulsar	Spin f (Hz)	Spin-down $\dot{f}$ (Hz s^{-1})	$h_0^{95\%}$ $/10^{-24}$	ϵ $/10^{-5}$
B0021 − 72C*	173.71	$+1.50 \times 10^{-15}$	4.3	16
B0021 − 72D*	186.65	$+1.19 \times 10^{-16}$	4.1	14
B0021 − 72F*	381.16	-9.37×10^{-15}	7.2	5.7
B0021 − 72G*	247.50	$+2.58 \times 10^{-15}$	4.1	7.5
B0021 − 72L*	230.09	$+6.46 \times 10^{-15}$	2.9	6.1
B0021 − 72M*	271.99	$+2.84 \times 10^{-15}$	3.3	5.0
B0021 − 72N*	327.44	$+2.34 \times 10^{-15}$	4.0	4.3
J0030 + 0451	205.53	-4.20×10^{-16}	3.8	0.48
B0531 + 21*	29.81	-3.74×10^{-10}	41	2100
J0711 − 6830	182.12	-4.94×10^{-16}	2.4	1.8
J1024 − 0719*	193.72	-6.95×10^{-16}	3.9	0.86
B1516 + 02A	180.06	-1.34×10^{-15}	3.6	21
J1629 − 6902	166.65	-2.78×10^{-16}	2.3	2.7
J1721 − 2457	285.99	-4.80×10^{-16}	4.0	1.8
J1730 − 2304*	123.11	-3.06×10^{-16}	3.1	2.5
J1744 − 1134*	245.43	-5.40×10^{-16}	5.9	0.83
J1748 − 2446C	118.54	$+8.52 \times 10^{-15}$	3.1	24
B1820 − 30A*	183.82	-1.14×10^{-13}	4.2	24
B1821 − 24*	327.41	-1.74×10^{-13}	5.6	7.1
J1910 − 5959B	119.65	$+1.14 \times 10^{-14}$	2.4	8.5
J1910 − 5959C	189.49	-7.90×10^{-17}	3.3	4.7
J1910 − 5959D	110.68	-1.18×10^{-14}	1.7	7.2
J1910 − 5959E	218.73	$+2.09 \times 10^{-14}$	7.5	7.9
J1913 + 1011*	27.85	-2.61×10^{-12}	51	6900
J1939 + 2134*	641.93	-4.33×10^{-14}	13	2.7
B1951 + 32*	25.30	-3.74×10^{-12}	48	4400
J2124 − 3358*	202.79	-8.45×10^{-16}	3.1	0.45
J2322 + 2057*	207.97	-4.20×10^{-16}	4.1	1.8

were performed. The black lines in Fig. 2 show marginalizations of the joint posterior from H1, H2, and L1, i.e.,

$$p(\boldsymbol{a}|\mathrm{H1, H2, L1}) \propto p(\boldsymbol{a})p(\mathrm{H1}|\boldsymbol{a})p(\mathrm{H2}|\boldsymbol{a})p(\mathrm{L1}|\boldsymbol{a}). \quad (3)$$

For three detectors of similar sensitivities and operational times, these coherent results would be approximately $\sqrt{3}$ times tighter than the individual results. The posteriors for ϕ_0 clearly highlight the relative coherence between the instruments and verify that joint methods can be used to set upper limits on our target pulsars.

Results.—We selected 28 targets from the ATNF pulsar catalogue [7]. For 18 of these, we obtained updated timing solutions from regular timing observations made at the Jodrell Bank Observatory using the Lovell and the Parkes telescopes, adjusted for a reference epoch centered on the epoch of the S2 run (starred pulsars in Table I). Details of the techniques that were used to do this can be found in [8]. We also checked that none of these pulsars exhibited a glitch during this period.

The list includes globular cluster pulsars (including isolated pulsars in 47 Tuc and NGC6752), the S1 target millisecond pulsar (J1939 + 2134), and the Crab pulsar (B0531 + 21). Although Table I shows only approximate pulsar frequencies and frequency derivatives, further phase corrections were made for pulsars with measured second derivatives of frequency. Timing solutions for the Crab were taken from the Jodrell Bank online ephemeris [9], and adjustments were made to its phase over the period of S2 using the method of [10].

The analysis used 910 h of data from H1, 691 h from H2, and 342 h from L1. There was no evidence of strong spectral contamination in any of the bands investigated, such as might be caused by an instrumental feature or a potentially detectable pulsar signal. A strong gravitational signal would generate a parameter PDF prominently peaked off zero with respect to its width, as for the hardware injections. Such a PDF would trigger a more detailed investigation of the pulsar in question. No such triggers occurred in the analysis of these data, and we therefore present upper limits.

The upper limits are presented as the value of h_0 bounding 95% of the cumulative probability of the marginalized strain PDF from $h_0 = 0$. The joint upper limit $h_0^{95\%}$ therefore satisfies

$$0.95 = \int_{h_0=0}^{h_0^{95\%}} dh_0 \iiint p(\boldsymbol{a}|\mathrm{H1, H2, L1}) d\iota d\psi d\phi_0, \quad (4)$$

consistent with [2]. The uncertainty in the noise floor estimate is already included, as outlined above.

The remaining uncertainties in the upper limit values of Table I stem from the calibration of the instrument and from the accuracy of the pulsar timing models. For L1 and H2, the amplitude calibration uncertainties are conservatively estimated to be 10% and 8%, respectively. For H1, the maximum calibration uncertainty is 18%, with typical values at the 6% level. Phase calibration uncertainties are negligible in comparison: less than 10° in all detectors. Biases due to pulsar timing errors are estimated to be 3% or less for J0030 + 0451, and 1% or less for the remaining pulsars (see [2] for a discussion of the effect of these uncertainties).

Discussion.—The improved sensitivity of the LIGO interferometers is clear from the strain upper limit for pulsar J1939 + 2134, which is more than a factor of 10 lower than was achieved with the S1 data [2]. In this analysis the lowest limit is achieved for pulsar J1910 − 5959D at the level of 1.7×10^{-24}, largely reflecting the lower noise floor around 200 Hz.

Table I also gives approximate limits to the ellipticities [3] of these pulsars from the simple quadrupole model

$$\epsilon \simeq 0.237 \frac{h_0}{10^{-24}} \frac{r}{1\ \mathrm{kpc}} \frac{1\ \mathrm{Hz}^2}{f^2} \frac{10^{45}\ \mathrm{g\,cm}^2}{I_{zz}}, \qquad (5)$$

where r is the pulsar's distance, which we take as the dispersion measure distance using the model of Taylor and Cordes [11], and I_{zz} its principal moment of inertia about the rotation axis, which we take as 10^{45} g cm^2.

As expected, none of these upper limits improves on those inferred from simple arguments based on the gravitational luminosities achievable from the observed loss of pulsar rotational kinetic energy. However, as discussed in the introduction, for pulsars in globular clusters such arguments are complicated by cluster dynamics, which the direct limits presented here avoid.

The result for the Crab pulsar (B0531 + 21) is within a factor of about 30 of the spin-down limit and over an order of magnitude better than the previous direct upper limit of [12]. The equatorial ellipticities of the four closest pulsars (J0030 + 0451, J2124 + 3358, J1024 − 0719, and J1744 − 1134) are constrained to be less than 10^{-5}.

Once the detectors operate at design sensitivity for a year, the observational upper limits will improve by more than an order of magnitude. The present analysis will also be extended to include pulsars in binary systems, significantly increasing the population of objects under inspection.

The authors gratefully acknowledge the support of the United States National Science Foundation for the construction and operation of the LIGO Laboratory and the Particle Physics and Astronomy Research Council of the United Kingdom, the Max-Planck-Society, and the State of Niedersachsen/Germany for support of the construction and operation of the GEO600 detector. The authors also gratefully acknowledge the support of the research by these agencies and by the Australian Research Council, the Natural Sciences and Engineering Research Council of Canada, the Council of Scientific and Industrial Research of India, the Department of Science and Technology of India, the Spanish Ministerio de Ciencia y Tecnologia, the John Simon Guggenheim Foundation, the Leverhulme Trust, the David and Lucile Packard Foundation, the Research Corporation, and the Alfred P. Sloan Foundation. This document has been assigned LIGO Laboratory Document No. LIGO-P040008-C-Z.

*Electronic address: http://www.ligo.org

[1] B. Abbott *et al.* (LIGO Scientific Collaboration), Nucl. Instrum. Methods Phys. Res., Sect. A **517/1-3**, 154 (2004).
[2] B. Abbott *et al.* (LIGO Scientific Collaboration), Phys. Rev. D **69**, 082004 (2004).
[3] P. Jaranowski, A. Królak, and B. Schutz, Phys. Rev. D **58**, 063001 (1998).
[4] B. J. Owen, Phys. Rev. Lett. (to be published).
[5] R. Dupuis, Ph.D. thesis, University of Glasgow, 2004.
[6] G. L. Bretthorst, *Lecture Notes in Statistics* (Springer-Verlag, Berlin, 1988), Vol. 48.
[7] www.atnf.csiro.au/research/pulsar/psrcat/.
[8] G. Hobbs, A. G. Lyne, M. Kramer, C. E. Martin, and C. Jordan, Mon. Not. R. Astron. Soc. **353**, 1311 (2004).
[9] www.jb.man.ac.uk/research/pulsar/crab.html.
[10] M. Pitkin and G. Woan, Classical Quantum Gravity **21**, S843 (2004).
[11] J. H. Taylor and J. M. Cordes, Astrophys. J. **411**, 674 (1993).
[12] T. Suzuki, in *First Edoardo Amaldi Conference on Gravitational Wave Experiments*, edited by E. Coccia, G. Pizzella, and F. Ronga (World Scientific, Singapore, 1995), p. 115.